COBEM 2023 27TH INTERNATIONAL CONGRESS OF MECHANICAL ENGENEERING

ABCM Brazilian Society of Mechanical Sciences and Engineering
27th ABCM International Congress of Mechanical Engineering
December 04-08, 2023, Florianópolis-SC, Brazil

COB-2023-1681
A STUDY ABOUT THE EFFECTS OF EXTENSIBILITY IN CANTILEVERED PIPES CONVEYING FLUID UNDER VIV USING A MODULAR MODELING METHODOLOGY

Daniel de Oliveira Tomin
Renato Maia Matarazzo Orsino
Celso Pupo Pesce
Offshore Mechanics Laboratory, Escola Politécnica, University of São Paulo, Av. Professor Lúcio Martins Rodrigues, Tv. 4, n. 434, São Paulo - SP, 05508-020, Brazil
daniel.tomin@usp.br, reorsino@usp.br, ceppesce@usp.br

Abstract. *The aim of this paper is to obtain two planar nonlinear reduced-order models of a relevant, but still underdiscussed topic in Fluid-Structure Interactions (FSI) literature, the slender cantilevered pipe conveying fluid subjected to vortex-induced vibrations due to external flow. One of the models considers an inextensible pipe and the other assumes extensibility consistently with the conservation of fluid mass inside the tube and Poisson's ratio. The mathematical formulation combines two classical FSI problems: i) The pipe ejecting fluid, which is an open system with an unique dynamical behaviour characterized by the presence of instability associated with a Hopf bifurcation, when a certain critical internal velocity threshold is reached (a previously related work showed that if this extensibility is considered when the ratio of axial and flexural stiffness is low, the critical velocity becomes higher when compared to inextensible models, also affecting the amplitude of the limit cycles encountered); ii) Cross-flow vortex-induced vibrations in flexible cylinders, using a phenomenological wake oscillator model with experimentally calibrated parameters for lower or upper branch tuning. The models are derived by applying the Extended Hamilton's Principle for nonmaterial volumes along with a modular based strategy, the Modular Modeling Methodology. This approach enables the consideration of nonlinearities associated with the extensibility, conservation of mass and VIV phenomenon by introducing redundant variables and subsystems, simplifying the mathematical manipulation and derivation to obtain the equations of motion of the original system through a recursive algorithm. Finally, some numerical simulations of VIV lock-in scenarios are highlighted and analyzed to compare the amplitudes obtained under discharging flow scenarios, considering both, an inextensible and an extensible pipe.*

Keywords: *Fluid-Structure Interactions, Vortex-Induced Vibrations, Pipe Conveying Fluid, Reduced-Order Modeling (ROM), Modular Modeling Methodology (MMM).*

1. INTRODUCTION

Fluid-structure interactions (FSI) have been the focus of several studies over the years, discussing phenomena of complex and multidisciplinary nature. The flexible slender pipe is a basic structural element that is an integral part of the extraction, ejection and transport of fluids, playing an important role in modern industry. Thus, the modeling of pipe vibrations due to fluid flow are a main point of scientific development.

The vibration induced by axial internal flow is an essential and fundamental problem of FSI. It is a open system (i.e., there is material transport across its boundary), that has a rich dynamical behavior characterized by instability of its equilibrium configuration after reaching a threshold value for the internal flow velocity, the critical velocity. Several authors proposed models with different hypotheses and boundary conditions, but the problem is usually treated as a cantilevered inextensible flexible pipe with internal plug flow (i.e., an uniform velocity profile at each cross section); therefore, the boundary layer is disregarded and the work of dissipative forces is assumed null. It is noteworthy that specific forms of variational principles associated with nonmaterial volumes should be utilized, taking into account momentum and kinetic energy transport terms.

FSI also includes the study of cross-flow vortex-induced vibrations (VIV) phenomenon in rigid and flexible cylinders introduced by external flow. VIV is related to the alternating shedding frequency of vortices in submerged bodies due to the separation of the boundary layer and Kelvin-Helmholtz instability. The vortices dynamically affect the pressure distribution along the surface of the body, originating oscillatory lift and drag forces that result in periodic cross and in-line motions. The modeling approaches have been progressing continuously, and include: i) Computational Fluid Dynamics (CFD), with high computational processing times; ii) Empirical models, in which the hydrodynamics forces are determined by experimental campaigns and correlations; iii) Phenomenological models, considering the motion coupling of specific nonlinear equations (with experimentally calibrated parameters), representing the wake dynamics.

For instance, one of the main practical applications of the pipe models is the analysis of the global dynamics of risers, in particular the so-called Seawater Intake Risers (SWIRs). SWIRs are risers that transport cold water from great depths, with the objective of increasing the energy efficiency of the refrigeration systems encountered in processing plants of floating production storage and offloading units (FPSOs). They are subjected to the combined effects of both axial internal flow and vortex-induced motion related to external flow.

Models that explore these concurrent phenomena are rarely found in the specialized literature, but this area has been addressed recently by researchers of the Offshore Mechanics Laboratory (LMO, in Portuguese) in recent papers and publications (such as Orsino *et al.* (2018a) and Orsino *et al.* (2022)) and a topic of a large experimental campaign detailed in Defensor Filho (2023) PhD thesis. In general, it can be stated that the combined effects are more pronounced when: the internal velocity is higher than critical velocity (related to dynamic Hopf bifurcations due to internal flow); and VIV lock-in scenarios, in which the wake oscillator dynamics is dominated by the structural vibrations associated with natural frequencies of the flexible modes.

The present work proposes the derivation of 2D reduced-order model for the cantilevered extensible submerged pipe ejecting fluid under VIV, in which the extensibility and conservation of mass are treated consistently, following a discussion elaborated in Tomin (2022) Master's thesis and Tomin *et al.* (2022). A correspondent inextensible model is also proposed. The VIV modeling considers a phenomenological approach based on Ogink and Metrikine (2010) and adapted in Orsino *et al.* (2018a). The extended Hamilton's Principle for nonmaterial volumes is utilized along with the Modular Modeling Methodology to derive the equations of motion (see Orsino (2016)). Moreover, from a Argand's type diagram (in some contexts, also known as root loci diagram) of the submerged pipe conveying fluid, the periods and instabilities of the flexible modes are evaluated. With the definition of set of parameters, some numerical simulations are defined in order to to obtain the maximum amplitude response of the free end. Subsequently, comparions between the inextensible and extensible models are presented.

This introduction is followed by five sections, with the last of them bringing concluding remarks. The second section describes the VIV phenomenological wake oscillator model utilized. In the third section, the dimensionless equations of motion for the proposed models are obtained through Galerkin's projection scheme associated with the extended Hamilton's Principle and the Modular Modeling Methodology. Finally, the discussions about the numerical simulations are in the fourth section.

2. VIV WAKE OSCILLATOR MODELING

VIV modeling was first based on the discrete problem of a rigid circular cylinder mounted on flexible supports with a single degree of freedom, a translation in the cross-flow direction. Later, discrete models with two degrees of freedom (cross and in-line motion) were developed. In the case of flexible circular cylinders, VIV becomes a phenomenon in which multimodal vibrations, parametric excitations, chaotic behavior, among others, are present.

Hydrodynamic loads due to VIV can considered using phenomenological models, such as the wake oscillator concept. This modeling strategy uses certain nonlinear equations that can represent the vortex wake dynamics. For instance, as adopted in works such as Facchinetti *et al.* (2004) and Ogink and Metrikine (2010).

In this paper, the model introduced in Ogink and Metrikine (2010) - which itself is a redevelopment of Facchinetti *et al.* (2004) - is utilized. The lift force from a stationary cylinder is $F_L = (1/2)\rho U^2 D C_L$, where ρ is the mass density of the fluid, U is the velocity of the external flow, D is the diameter of the pipe and C_L is the force coefficient. From Ogink and Metrikine (2010), the limit-cycle oscillatory behavior can be obtained through the Van der Pol equation

$$\frac{\partial^2 Q}{\partial t^2} + \epsilon_s \omega_s (Q^2 - 1)\frac{\partial Q}{\partial t} + \omega_s^2 Q = 0. \tag{1}$$

Indeed, assume that t is the time, Q is the wake variable, ω_s is the vortex-shedding frequency (related to the Strouhal number St) and ϵ_s is a experimentally calibrated parameter. The lift coefficient can be related to the wake variable Q with

$$C_L = \frac{\hat{C}_L}{\hat{Q}} Q, \tag{2}$$

in which $\hat{C}_L$ is the amplitude of the lift coefficient and $\hat{Q} = 2$ is the amplitude of the limit cycle of the unforced Van der Pol oscillator.

For a 1-DOF rigid cylinder, the equations of motion of the cross-flow displacement $y(t)$ and the wake variable $Q(t)$ could be adapted using a acceleration coupling term associated with an empirical parameter A that correlates the structural vibrations with the fluid hydrodynamics. Consider the following,

$$(m_r + m_{ar})\frac{\partial^2 y}{\partial t^2} + c_r \frac{\partial y}{\partial t} + k_r y = \frac{1}{2}\rho U^2 D C_Y, \tag{3}$$

and

$$\frac{\partial^2 Q}{\partial t^2} + \epsilon_s \omega_s (Q^2 - 1)\frac{\partial Q}{\partial t} + \omega_s^2 Q = \frac{A}{D}\frac{\partial^2 y}{\partial t^2}, \tag{4}$$

where m_r, m_{ar}, c_r, k_r and C_Y represent, respectively, the mass, the added mass, the damping, the structural stiffness and the hydrodynamic force coefficient. The experimental parameters A and ϵ_s are different according to the investigated amplitude response in the upper or lower VIV branches.

As the velocity of cylinder is about the same magnitude of the free-stream flow velocity, the hydrodynamic force coefficient C_Y can be written in terms of the lift C_L and drag C_D force coefficients of stationary circular cylinders experimental data using

$$C_Y = \frac{C_D \sin(\theta) + C_L \cos(\theta)}{\cos^2(\theta)}. \tag{5}$$

Consider θ as the angle between the direction of U and the relative velocity $U - \partial y/\partial t$. Thus,

$$\sin(\theta) = -\frac{\frac{\partial y}{\partial t}}{\sqrt{U^2 + \left(\frac{\partial y}{\partial t}\right)^2}},\ \cos(\theta) = \frac{U}{\sqrt{U^2 + \left(\frac{\partial y}{\partial t}\right)^2}} \tag{6}$$

Following Orsino *et al.* (2018a), the VIV phenomenological model presented in Ogink and Metrikine (2010) is modified for the modeling of the flexible submerged pipe conveying fluid in the context of Modular Modeling Methodology in the next section.

3. SUBMERGED EXTENSIBLE PIPE CONVEYING FLUID UNDER VIV

Assume a cantilevered flexible pipe constituted by an linear elastic material axially conveying incompressible flow as represented in Fig. 1. The pipe is also submerged in a fluid with a constant external free-stream velocity, so that votex-induced vibrations in the cross-flow direction are induced.

The center of the clamped cross section is adopted as the origin of a coordinate system (x, y, z) with corresponding unit vectors $(\mathbf{e_1}, \mathbf{e_2}, \mathbf{e_3})$, defining an orthonormal basis. The pipe moves in the xz-plane and the external velocity $U\mathbf{e}_2$ is ortogonal to that plane. The x-coordinate in the reference configuration is x_0 which is parallel to the length of the tube and aligned with the local gravitational field $g\mathbf{e}_1$. The displacements are $u = x - x_0$ and $w = z - z_0$ and $w = z$ and arc-length coordinate is s.

Let $(\,)' = \partial(\,)/\partial x_0$. Consider:

- The pipe is modeled as a Euler-Bernoulli beam in the xz-plane assuming geometric nonlinearies. The position vector is $\mathbf{R} = (x_0+u, 0, w)$, the axial strain is $\varepsilon = 1+u'+(1/2)u'^2+(1/2)w'^2$, the instantaneous tangent unit vector is $\boldsymbol{\tau} = (1/(1+\varepsilon))(1+u', 0, w')$, the normal unit vector in the xz-plane is $\mathbf{n} = \mathbf{e}_2 \times \boldsymbol{\tau} = (1/(1+\varepsilon))(w', 0, -1-u')$ and the curvature is $\kappa = (w''(1+u') - w'u'')/(1+\varepsilon)^3$;
- Let L denote the unstretched pipe length, D its diameter, EI its bending stiffness, EA its axial stiffness, ν its Poisson's ratio and $b = 1 - 2\nu$ its volume change rate. The linear mass is m, the linear mass of displaced fluid is m_d and the added mass per unit length is m_a (associated with potential flow theory[1]);
- The internal fluid linear mass is M and the internal flow velocity is $V\boldsymbol{\tau}$. The present work adopts a generalized expression for V which is consistent with the conservation of mass for incompressible flows in extensible pipes with plug flow hypothesis that was utilized in Tomin (2022) and Tomin *et al.* (2022)

$$V = V_0 - \int_0^{x_0} \frac{b(1+\varepsilon)}{1+b\varepsilon}\frac{\partial \varepsilon}{\partial t}\,\mathrm{d}x_0, \tag{7}$$

  where V_0 is the velocity at the fixed end ($x_0 = 0$).
- The external fluid mass density is ρ and free-stream velocity is $U\mathbf{e}_2$. C_n is the force coefficient due to VIV.

[1] Assumption from the phenomenological model formulated in Ogink and Metrikine (2010).

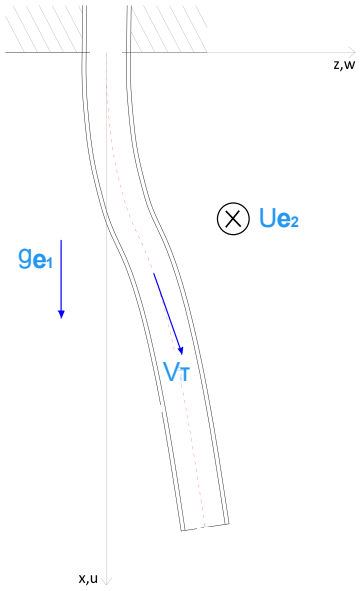

Figure 1: The 2D model of the submerged extensible pipe conveying fluid. Adapted from Tomin (2022).

3.1 On the use of the Extended Hamilton's Principle for nonmaterial volumes

A material volume or a closed system is a fictional volume that always contains all of the material body, following the motion of the particles located in its surface. Therefore, no transport of matter is present. On the other hand, a nonmaterial volume or an open system is a fictional body which only instantly coincides with a region defined by the material particles, so not all the particles are accounted within its volume and material transport may occur through the open boundary.

In Analytical Mechanics, classic variational formulations are generally well formulated for closed systems; however, extended forms of these expressions - with complementary terms accounting for the material transport - are utilized for open systems. Let δ be a variation according to Variational Calculus. The Extended Hamilton's Principle for nonmaterial volumes is derived in Casetta and Pesce (2013) and is written

$$\int_{t_1}^{t_2} \left[\delta T_u + \delta W + \delta W_M + \delta W_{KE}\right] \, \mathrm{d}t = 0. \tag{8}$$

in which T_u is the kinetic energy, δW is the virtual work of the conservative and nonconservative forces, δW_M and δW_{KE} are the additional terms related to the transport of momentum and kinetic energy, respectively.

Consider $\dot{(\,)} = \partial(\,)/\partial t$. In the present case, the kinetic energy T_u includes the tube and conveyed fluid,

$$T_u = \frac{m}{2}\int_0^L \dot{\mathbf{R}}\cdot\dot{\mathbf{R}}\,\mathrm{d}x_0 + \frac{M}{2}\int_0^L \left(\dot{\mathbf{R}} + V\boldsymbol{\tau}\right)\cdot\left(\dot{\mathbf{R}} + V\boldsymbol{\tau}\right)\,\mathrm{d}x_0. \tag{9}$$

The virtual work $\delta W = -\delta P + \delta W_{NC}$ is separated in the variation of potential energy P, related to the strain energy and the gravitational field, and the virtual work of nonconservative forces δW_{NC} for the hydrodynamics forces and added mass (dissipative and inner pressure forces are not considered in the modeling)

$$P = \frac{EA}{2}\int_0^L \varepsilon^2\,\mathrm{d}x_0 + \frac{EI}{2}\int_0^L (1+\varepsilon)^2\kappa^2\,\mathrm{d}x_0 - (m+M-m_d)\int_0^L \mathbf{g}\cdot\mathbf{R}\,\mathrm{d}x_0, \tag{10}$$

$$\delta W_{NC} = \int_0^L \left(\frac{1}{2}\rho D U^2 C_n \mathbf{n} - m_a\ddot{\mathbf{R}}\right)\cdot\delta\mathbf{R}\,\mathrm{d}x_0. \tag{11}$$

An expression for the force coefficient C_n is derived with the formulation found in Ogink and Metrikine (2010) and adapted in Orsino *et al.* (2018a). From Equations (2) and (5),

$$C_n = \frac{C_D\sin\theta + \frac{\hat{C}_L}{\hat{Q}}Q\cos\theta}{\cos^2\theta}. \tag{12}$$

In this case, the projection of the velocity $\dot{\mathbf{R}}$ in the direction of the unit vector $\mathbf{n}$ is utilized

$$\sin(\theta) = -\frac{\dot{\mathbf{R}} \cdot \mathbf{n}}{\sqrt{U^2 + \left(\dot{\mathbf{R}} \cdot \mathbf{n}\right)^2}}, \; \cos(\theta) = \frac{U}{\sqrt{U^2 + \left(\dot{\mathbf{R}} \cdot \mathbf{n}\right)^2}}, \tag{13}$$

and considering a similar modified version of Equation (4) for flexible cylinders

$$\ddot{Q} + \epsilon_s \omega_s (Q^2 - 1)\dot{Q} + \omega_s^2 Q = \frac{A}{D}\ddot{\mathbf{R}} \cdot \mathbf{n}. \tag{14}$$

Assume that q_i are the generalized coordinates of the discretized problem. The transport terms are not identically null only if $x_0 = L$ (see Tomin (2022))

$$\delta W_M = -MV \left[\left(\dot{\mathbf{R}} + V\boldsymbol{\tau} \right) \cdot \left(\frac{\partial \dot{\mathbf{R}}}{\partial \dot{q}_i} + \boldsymbol{\tau} \frac{\partial V}{\partial \dot{q}_i} \right) \right] (\boldsymbol{\tau} \cdot \boldsymbol{\tau}) \, \delta q_i \Big|_{x_0 = L} \tag{15}$$

$$\delta W_{KE} = \frac{M}{2} \frac{\partial V}{\partial \dot{q}_i} \left[\left(\dot{\mathbf{R}} + V\boldsymbol{\tau} \right) \cdot \left(\dot{\mathbf{R}} + V\boldsymbol{\tau} \right) \right] (\boldsymbol{\tau} \cdot \boldsymbol{\tau}) \, \delta q_i \Big|_{x_0 = L} \tag{16}$$

Now let $\dot{(\,)} = \partial(\,)/\partial\tau$ and $(\,)' = \partial(\,)/\partial\xi$. Consider the following dimensionless quantities of Table 1 and redundant variables of Table 2 to rewrite the Extended Hamilton's Principle and hide some nonlinearities present in the expressions.

Table 1: Dimensionless quantities.

Dimensionless parameter	**Symbol**	**Definition**
Undeformed axial coordinate	ξ	$\frac{x_0}{L}$
Axial and transversal displacements	η, ζ	$\frac{u}{L}$, $\frac{w}{L}$
Time	τ	$\left(\frac{EI}{M+m}\right)^{1/2} \frac{t}{L^2}$
Axial and flexural stiffness ratio	α	$\frac{EA}{EI}L^2$
Internal and external flow velocities	v, u	$\left(\frac{M}{EI}\right)^{1/2} V_0 L$, $\left(\frac{M+m}{EI}\right)^{1/2} UL$
Mass ratios	β, β_a, β_d	$\frac{M}{M+m}$, $\frac{m_a}{M+m}$, $\frac{m_d}{M+m}$
Gravitational and flexural stiffness ratio	γ	$\frac{M+m}{EI}gL^3$
Inverse of the pipe aspect ratio	ϵ_a	$\frac{D}{L}$
Vortex-shedding frequency	Ω_s	$\left(\frac{M+m}{EI}\right)^{1/2} \omega_s L^2 = \frac{2\pi u}{\epsilon_a} St$

Table 2: Redundant variables.

Variable	Expression
Axial strain	$\hat{\varepsilon} = \eta' + \frac{1}{2}\eta'^2 + \frac{1}{2}\zeta'^2$
Curvature	$\hat{\kappa} = \frac{\zeta''(1+\eta') - \zeta'\eta''}{(1+\hat{\varepsilon})^2}$
Tangent unit vector	$\hat{\tau}_\eta = \frac{1+\eta'}{1+\hat{\varepsilon}}, \hat{\tau}_\zeta = \frac{\zeta'}{1+\hat{\varepsilon}}$
Internal velocity	$\dot{\hat{\Psi}} = \left[\frac{b(1+\hat{\varepsilon})}{1+b\hat{\varepsilon}}\right]\dot{\hat{\varepsilon}}, \dot{\hat{V}} = v\beta^{-1/2} - \int_0^\xi \dot{\hat{\Psi}}\,\mathrm{d}\xi$
Force coefficient	$\dot{\hat{C}}_n = \frac{C_D \frac{\dot{\eta}\hat{\tau}_\zeta - \dot{\zeta}\hat{\tau}_\eta}{\sqrt{u^2+\left(\dot{\eta}\hat{\tau}_\zeta - \dot{\zeta}\hat{\tau}_\eta\right)^2}} + \frac{\hat{C}_L}{\hat{Q}} Q \frac{u}{\sqrt{u^2+\left(\dot{\eta}\hat{\tau}_\zeta - \dot{\zeta}\hat{\tau}_\eta\right)^2}}}{\left(\frac{u}{\sqrt{u^2+\left(\dot{\eta}\hat{\tau}_\zeta - \dot{\zeta}\hat{\tau}_\eta\right)^2}}\right)^2}$

3.2 Modular Modeling Methodology

Following similar problems treated in Orsino and Pesce (2018), Orsino *et al.* (2018b) and Orsino *et al.* (2022), a reduced-order model is obtained with a Galerkin discretization scheme for the application of the Modular Modeling Methodology (MMM) technique. The fixed end of the pipe implies that $\eta(0,\tau) = 0,\ \zeta(0,\tau) = 0,\ \zeta'(0,\tau) = 0$, so a family of functions which identically satisfies these boundary conditions is adopted. The chosen projection functions are the nondimensional natural modes of clamped-free Euler-Bernoulli beam

$$h_i(\xi) = \cosh\Lambda_i\xi - \cos\Lambda_i\xi - \sigma_i(\sinh\Lambda_i\xi - \sin\Lambda_i\xi), \tag{17}$$

where $\sigma_i = (\sinh\Lambda_i - \sin\Lambda_i)/(\cosh\Lambda_i + \cos\Lambda_i)$ and each Λ_i results from the characteristic equation $\cos\Lambda_i\cosh\Lambda_i = -1$.

Assume that Q is a function of time and of the undeformed coordinate of the pipe. As lock-in scenarios are the main focus, the oscillations of the wake are dominated by the motion of the structure; consequently, the same projection functions are employed for the discretization of the cartesian variables η, ζ and the wake variable Q. Thus,

$$\eta(\xi,\tau) \cong \sum_{i=1}^{N} h_i(\xi)\eta_i(\tau),\ \zeta(\xi,\tau) \cong \sum_{i=1}^{N} h_i(\xi)\zeta_i(\tau),\ Q(\xi,\tau) \cong \sum_{i=1}^{N} h_i(\xi)Q_i(\tau). \tag{18}$$

The redundant variables of Table 2 are also discretized

$$\begin{aligned}
&\hat{\varepsilon}(\xi,\tau) \cong \sum_{i=1}^{N} h_i'(\xi)\hat{\varepsilon}_i(\tau),\ \hat{\tau}_\eta(\xi,\tau) \cong 1 + \sum_{i=1}^{N} h_i'(\xi)\hat{\tau}_{\eta i}(\tau),\ \hat{\tau}_\zeta(\xi,\tau) \cong \sum_{i=1}^{N} h_i'(\xi)\hat{\tau}_{\zeta i}(\tau),\ \hat{\kappa}(\xi,\tau) \cong \sum_{i=1}^{N} h_i''(\xi)\hat{\kappa}_i(\tau),\\
&\dot{\hat{\Psi}}(\xi,\tau) \cong \sum_{i=1}^{N} h_i'(\xi)\dot{\hat{\Psi}}_i(\tau,),\ \dot{\hat{V}}(\xi,\tau) \cong v\beta^{-1/2} + \sum_{i=1}^{N} h_i(\xi)\dot{\hat{V}}_i(\tau),\ \dot{\hat{C}}_n(\xi,\tau) \cong \sum_{i=1}^{N} h_i'(\xi)\dot{\hat{C}}_{ni}(\tau).
\end{aligned} \tag{19}$$

Using the Galerkin discretization procedure including the original and redundant variables, the nonlinear ODEs of the so-called relaxed model are derived, which does not represent the dynamics of the original system. In order to obtain the compatible equations of motion, the MMM algorithm states that the definitions of the redundant variables can be interpreted as constraints that must be enforced *a posteriori* in positions along the structure according to the number of projection functions selected. These points are labeled the collocation points.

In the extensible model, the expressions of Table 2 are utilized; however, when the inextensible model is considered, the complementary equation below in addition to the expressions in Tab. 2 are contemplated

$$\hat{\varepsilon} = 0, \tag{20}$$

which is related to the inextensibility condition of the dimensionless axial strain $\hat{\varepsilon} = \eta' + (1/2)\eta'^2 + (1/2)\zeta'^2 = 0$.

Therefore, if the generalized coordinates vector is $\mathbf{q}^\top = (\eta_i, \zeta_i, Q_i, \hat{\varepsilon}_i, \hat{\tau}_{xi}, \hat{\tau}_{zi}, \hat{\kappa}_i, \hat{\Psi}_i, \hat{V}_i, \hat{C}_{ni})$ for $i = 1, 2, \ldots, N$, and the discretized forms of the constraint equations are imposed at $\xi = \xi_i$ points, they could be written in the matrix form

$$\mathbf{A}\ddot{\mathbf{q}} = \mathbf{b}(\tau, \mathbf{q}, \dot{\mathbf{q}}). \tag{21}$$

The relaxed nonlinear equations of motion are also written in matrix form

$$\mathbf{M}\ddot{\mathbf{q}} = \mathbf{f}(\tau, \mathbf{q}, \dot{\mathbf{q}}). \tag{22}$$

Now, consider the projection operator $\mathbf{S}$ whose image is the kernel of the Jabobian matrix $\mathbf{A}$. Per MMM algorithm, the equations of motion for the original system can be expressed as follows

$$\begin{bmatrix} \mathbf{S}^\top \mathbf{M} \\ \mathbf{A} \end{bmatrix} \ddot{\mathbf{q}} = \begin{bmatrix} \mathbf{S}^\top \mathbf{f} \\ \mathbf{b} \end{bmatrix}. \tag{23}$$

Figure 2 summarizes the aforementioned procedures for the derivation of the extensible and inextensible models. The redundant variables make it possible to avoid the presence of nonlinear terms in the derivation of the relaxed model, since they are included a posteriori as constraints, simplifying the algebraic derivation, manipulation and coupling of terms in the modeling. The constraint equations are utilized without any polynomial approximation. Some disadvantages of this technique include: i) A large number of generalized coordinates associated with the redundant variables and the chosen projection functions, which increase the processing time of the linear or nonlinear analyzes; ii) Due to the complexity of the matrix $\mathbf{A}$ and matrix $\mathbf{S}$, the equations of motion can not be obtained in a explicit form. So, these projection operators are evaluated in each the time step of the numerical integration; iii) One important aspect is to investigated the relative imposition of the constraints not only in the collocation points ξ_i, but also in the continuum (in this case, the interval $0 \leq \xi \leq 1$).

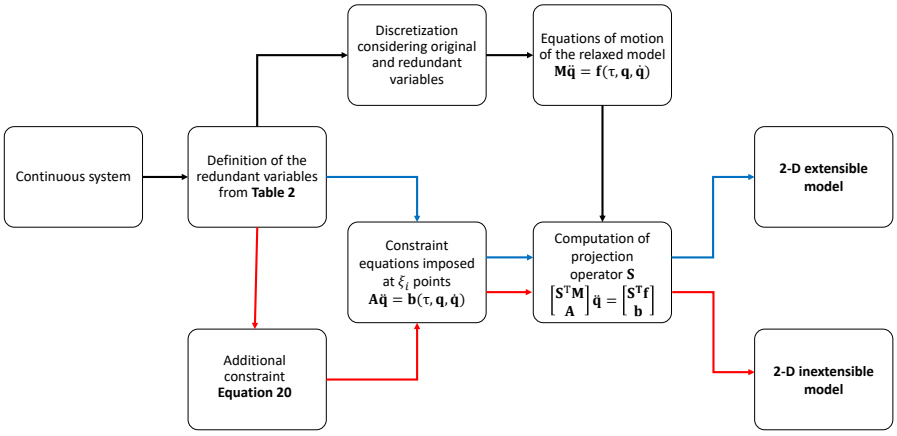

Figure 2: Flowchart of the application of MMM. Blue arrows only represent steps related to the derivation of the extensible model. Red arrows for the inextensible model. Black arrows for both models.

4. NUMERICAL SIMULATIONS

Some parameters for the numerical simulations are selected according to the values presented in Ogink and Metrikine (2010) for upper or lower branch tuning. In addition, Poisson's ratio ν, the dimensionless gravitational parameter γ and the axial and flexural stiffness ratio α are determined by the extent of the values investigated in Tomin (2022) and Tomin *et al.* (2022). These works showed that for relatively low axial and flexural stiffness ratio ($\alpha \approx 1000$), the difference between the critical velocities of the extensible and inextensible models is significant. See Table 3.

Table 3: Dimensionless parameters for upper or lower branch tuning. Potential flow hypothesis is associated with β_a.

Parameter	**Value**	**Source**	**Parameter**	**Value**	**Source**
α	1000	[1]	C_D	1.1856	[2]
ν	0.5	[1]	$\hat{C}_L$	0.3842	[2]
γ	100	[1]	$\hat{Q}$	2	[2]
β	0.2	[2]	ϵ_s	0.05* or 0.7**	[2]
ϵ_a	0.02	[2]	A	4* or 12**	[2]
$\beta_d = \beta_a$	0.4167	[2]	St	0.1932	[2]

[1]Tomin (2022) and Tomin *et al.* (2022) [2]Ogink and Metrikine (2010)
*Upper branch **Lower branch

As illustrated in Figure 3, root loci (Argand's) diagrams of the submerged pipe conveying fluid models are obtained through a linearization procedure and, subsequently, the eigenvalues λ_i are evaluated with Lyapunov's indirect method. Each value of the internal velocity v changes the natural periods T_i associated with the transversal and axial modes. The mode curves are labeled using the descending order of T_i calculated at $v = 0$ and according to the considered model: in the extensible graphs, both the axial and transversal modes are shown, whereas only the transversal modes are present in the inextensible case. A dashed line represents the position of the critical velocity v_c in each root loci.

For the selected parameters, the inextensible pipe becomes unstable for internal flow velocities above $v_c \approx 8.6$, with a Hopf bifurcation appearing in the curve of the second transversal mode. Whereas, the extensible model is unstable for internal flow velocities above $v_c \approx 10.0$ in the third transversal mode. Qualitatively, the instability is the same, but the extensible model leads to a significantly higher critical velocity, even changing the position of the Hopf bifurcation between the transversal modes.

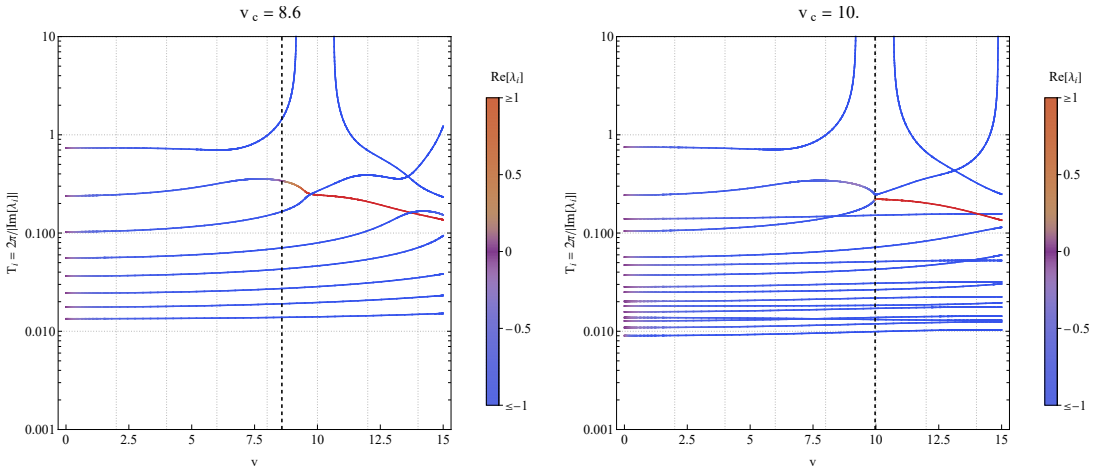

Figure 3: Root loci $T_i = 2\pi/\left|\mathrm{Im}[\lambda_i]\right| \times v$. Color scale: $\mathrm{Re}[\lambda_i]$. The red color denotes instability according to Lypunov's indirect method. (Left) The inextensible model. (Right) The extensible model.

The equations of motion obtained through Equation (23) are numerically integrated to study the influence of the combined effects of internal and external flows with $N = 8$ projection functions. The initial simulations consider VIV lock-in scenarios in the upper branch tuned to the transversal mode in which a Hopf bifurcation occurs in Figs. 3. Therefore, the external velocity u is tuned to the second and third transversal modes using the expression $u = \epsilon_a |Im[\lambda_i]|/2\pi St = \epsilon_a/T_i St$. Considering steady-state, diagrams displaying the amplitude of the free end transversal displacements $A_\zeta(\xi = 1)$ as a function of v - normalized by the external diameter of the pipe - are in Fig. 4. Dashed lines represent the calculated critical velocities v_c of the inextensible and extensible models.

At $v = 0$, the pipes amplitude is about 1.4 of its diameter. In both cases, the models experience some mitigation when $v < v_c$, with a decrease in the amplitude as v becomes higher, reaching a minimum between $4.5 < v < 6.5$; then, as v increases, the amplitude follows. This effect is present specially in the second mode diagram (at $v = 5.5$, the amplitude is 0.65 of the diameter), but less noticeable in the third mode tuning (at $v = 6.0$, the amplitude is 1.0 of the diameter). In the interval below the critical velocity threshold $v_c = 8.6$ of the inextensible case, the results of both set of simulations are relatively close; however, amplification already exists concerning the second mode (at $v = 8$, the amplitude is 1.8 of the diameter).

When $8.6 < v < 10.0$ - i.e., below the critical velocity of the extensible model and above the inextensible pipe - in the second mode tuning, the amplitudes are amplified when compared to $v = 0$, but the inextensible values are significantly higher than the extensible values. In the third mode tuning, the inextensible amplitude becomes higher only at $v = 9.5$. It is important to note that this study is of qualitative nature, as the amplitudes become sufficiently large to destroy the wake dynamics of the self-regulated VIV phenomenon, in accordance with the limitations of phenomenological models.

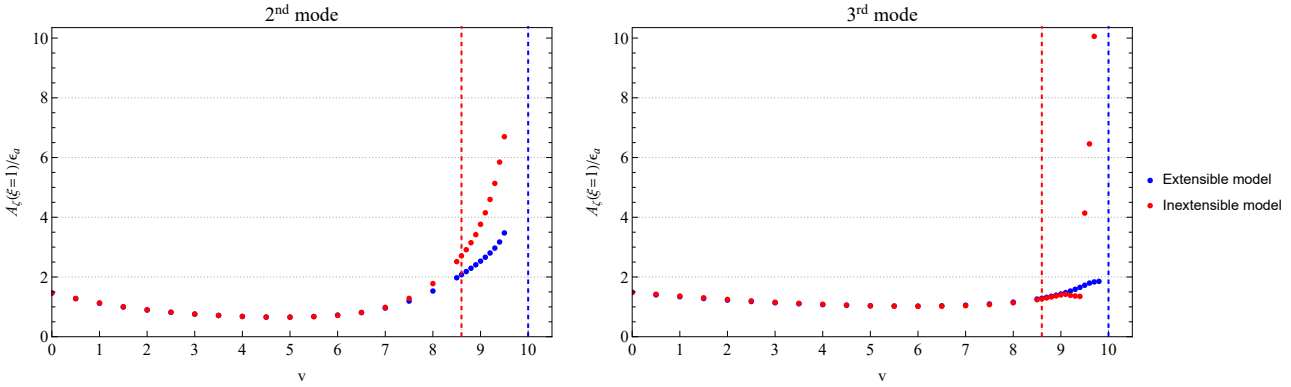

Figure 4: Amplitudes of the free end with upper branch tuning. The red dashed line is the critical velocity of the inextensible model and the blue is the critical velocity of the extensible model. (Left) Second transversal mode tuning. (Right) Third transversal mode tuning.

By fixing $v = 8.7$, the frequency of the second transversal mode is $f_{N,2} \approx 3.0$ for both pipe models and the mode shape is $\phi_{N,2}(\xi)$. Consider the associated reduced velocity $u_{R,2} = u/f_{N,2}\epsilon_a$. To obtain the classical VIV amplitude curve, the simulation is decomposed into a set of mode shapes with a projection operator, highlighting the participation of each shape in the response. Figure 5 shows the the amplitude $A_{N,2}$ of the second transversal mode and the period ratio $f/f_{N,2}$ (f is the dominant frequency of the analysed signal) as a function of the reduced velocity $u_{R,2}$.

When both VIV and internal flow supercritical effects are considered, the maximum mode amplitude is about 2.4 of the diameter in the inextensible model and 1.9 in the extensible model. In general, as expected, the amplitudes are higher considering inextensible pipe than the extensible pipe.

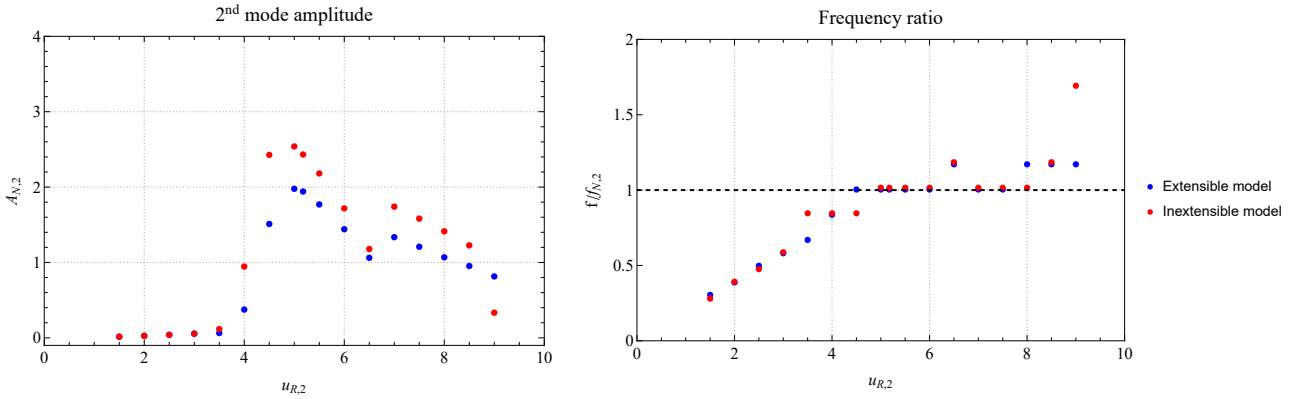

Figure 5: Amplitude and frequency ratio as a function of the reduced velocity $u_{R,2} = u/f_{N,2}\epsilon_a$ with $v = 8.7$. Upper branch parameters were utilized in the interval $0 \leq u_{R,2} \leq 6.5$ and lower branch in $u_{R,2} > 6.5$. (Left) Amplitude of the second mode calculated with a projection operator. (Right) Frequency ratio $f/f_{N,2}$. Close scenarios to the dashed line represent the lock-in responses.

5. CONCLUDING REMARKS

This work proposed a formulation and analysis of a planar nonlinear reduced-order model for submerged extensible pipes conveying fluid under vortex-induced vibrations (VIV). To derive the equations of motion, the extended Hamilton's Principle for nonmaterial volumes - which accounts for the material transport through open boundary - and an algorithm based on Modular Modeling Methodology (MMM) were utilized. This modeling strategy allowed the coupling of the extensible pipe conveying fluid model (consistently with the conservation of mass inside the pipe, already discussed in Tomin (2022) and Tomin *et al.* (2022)) with a phenomenological wake oscillator model developed by Ogink and Metrikine (2010) and adapted for MMM by Orsino *et al.* (2018a). The use of redundant variables simplifies the mathematical

manipulation of nonlinear terms, which can be interpreted as constraints that must be enforced *a posteriori* along the length of the pipe.

The initial numerical simulations explored lock-in scenarios with upper branch tuning and evaluates the dynamical behaviors of the inextensible and extensible models, specially concerning the distinct critical velocities encountered. When only VIV is considered, the maximum transversal displacement is about 1.4 of its diameter; if a pre-critical scenario ($v < v_c$) is investigated, this amplitude is usually mitigated, but some amplification is present for values close to the critical velocity in the second mode tuning; and if $8.6 < v < 10.0$, there is an amplification, but the amplitudes of the inextensible pipe are considerable higher than the extensible pipe in the second mode tuning and in the third mode tuning when $v \geq 9.5$. If the internal velocity is fixed $v = 8.7$, classical VIV amplitude curves - as a function of reduced velocity - are obtained, showing similar results between the models. The extensibility condition increases the stability of the pipe conveying fluid system, leading to significantly different amplitudes in the simulations, which combines the effects of both the internal and external flows.

An extension of this model to a three dimensional one is presently under way. After this task is accomplished, validation is planned to be done by comparing numerical data with the results from the experimental campaign detailed in Defensor Filho (2023). That experimental study was carried out within the scope of a SWIR R&D research project, in which reinforced flexible hoses - equipped with a ballast at the free end - were tested in various dynamic scenarios, including the concomitant action of internal flow and VIV. An immense database was generated, useful for further validation and verification of analytical and phenomenological models.

6. ACKNOWLEDGEMENTS

The São Paulo State Research Foundation (FAPESP) is gratefully acknowledged, for having supported the whole development of the basic mathematical formalism, since 2012, through Grants 2012/10848-4, 2013/02997-2, 2016/09730-0 and for the first author on-going PhD scholarship, 2023/03135-6, linked to the Thematic Project "Nonlinear Dynamics applied to Engineering Systems", process no. 2022/00770-0. The authors also acknowledge the National Council for Scientific and Technological Development (CNPq) for C. Pesce's Research Grant 307995/2022-4.

7. REFERENCES

Casetta, L. and Pesce, C.P., 2013. "The generalized Hamilton's principle for a non-material volume". *Acta Mechanica*, Vol. 224, No. 4, pp. 919–924. ISSN 00015970. doi:10.1007/s00707-012-0807-9.

Defensor Filho, W.A., 2023. *An experimental investigation with vertically suspended flexible pipes conveying water in aspirating and discharging conditions in a towing tank*. Ph.D. thesis, University of São Paulo.

Facchinetti, M., de Langre, E. and Biolley, F., 2004. "Coupling of structure and wake oscillators in vortex-induced vibrations." *Journal of Fluids and Structures*, Vol. 19, No. 2, pp. 123–140. doi:10.1016/j.jflui dstructs.2003.12.004.

Ogink, R. and Metrikine, A., 2010. "A wake oscillator with frequency dependent coupling for the modeling of vortex-induced vibration". *Journal of Sound and Vibration*, Vol. 329, No. 26, pp. 5452–5473. doi:10.1016/j.jsv.2010.07.008.

Orsino, R.M.M., Pesce, C.P. and Franzini, G.R., 2018a. "Cantilevered pipe ejecting fluid under VIV: an investigation based on a planar nonlinear reduced-order model". *Journal of the Brazilian Society of Mechanical Sciences and Engineering*, Vol. 40, No. 11. ISSN 18063691. doi:10.1007/s40430-018-1467-z.

Orsino, R.M.M., 2016. *A contribution on modeling methodologies for multibody systems*. Ph.D. thesis, Universidade de São Paulo.

Orsino, R.M.M. and Pesce, C.P., 2018. "Modular methodology applied to the nonlinear modeling of a pipe conveying fluid: A novel finite element method based approach". *Journal of the Brazilian Society of Mechanical Sciences and Engineering*, Vol. 40, No. 2. ISSN 18063691. doi:10.1007/s40430-018-0994-y.

Orsino, R.M.M., Pesce, C.P. and Franzini, G.R., 2018b. "A 3D non-linear reduced order model for a cantilevered pipe ejecting fluid under VIV". *Proceedings of 9th International Symposium on Fluid-Structure Interactions, Flow-Sound Interactions, Flow-Induced Vibration & Noise - FIV2018*.

Orsino, R.M.M., Pesce, C.P., Toni, F.G., Defensor Filho, W.A. and Franzini, G.R., 2022. "A 3D nonlinear reduced order model of a cantilevered aspirating pipe under VIV". In *Advances in Nonlinear Dynamics: Proceedings of the Second International Nonlinear Dynamics Conference - NODYCON 2021*. Vol. 1.

Tomin, D.O., 2022. *Dinâmica de tubos extensíveis com escoamento interno: uma abordagem via Mecânica Analítica*. Master's thesis, University of São Paulo.

Tomin, D.O., Orsino, R.M.M. and Pesce, C.P., 2022. "Cantilevered extensible pipes conveying fluid: a consistent reduced-order modeling via the extended Hamilton's principle for nonmaterial volumes". In *10th European Nonlinear Dynamics Conference – ENOC2022*.

8. RESPONSIBILITY NOTICE

The authors are solely responsible for the printed material included in this paper.